Clim. Past Discuss., doi:10.5194/cp-2016-53, 2016
Manuscript under review for journal Clim. Past
Published: 26 May 2016

Climate of the Past Discussions

Sulphur-rich volcanic eruptions triggered extreme hydrological events in Europe since AD 1850

Cristina Di Salvo[1] Gianluca Sottili[1#]

[1] Istituto di Geologia Ambientale e Geoingegneria IGAG-CNR, Rome [Italy].
#Correspondence to: gianluca.sottili@uniroma1.it

Keywords: sulphate aerosols, volcanic forcing, European climate, hydrological cycle

Clim. Past Discuss., doi:10.5194/cp-2016-53, 2016
Manuscript under review for journal Clim. Past
Published: 26 May 2016

Climate of the Past
Discussions

Abstract. Volcanic and anthropogenic aerosols, by reflecting solar radiation and acting as cloud condensation nuclei, play a key role in the global climate system. Given the contrasting microphysical and radiative effects of SO_2 on rainfall amounts and intensities, the combined effects of these two factors are still poorly understood. Here, we show how concentrations of volcanic sulphate aerosols in the atmosphere, as derived from Greenland ice core records, are strictly correlated with dramatic variations of hydrological cycle in Europe. Specifically, since the second half of the 19^{th} century, the intensity of extreme precipitations in Western Europe, and associated river flood events, changed significantly during the 12-24 months following sulphur-rich eruptions. During the same period, volcanic SO_2 exerts divergent effects in central and Northern Europe, where river flow regimes are affected, in turn, by the substantial reduction of rainfall intensity and earlier occurrences of ice break-up events. We found that the high sensitivity of North Atlantic Sea Surface Temperature (SST) and North Atlantic Oscillation (NAO) to atmospheric SO_2 concentrations reveals a complex mechanism of interaction between sulphur-rich eruptions and heat exchange between Ocean and atmosphere with substantial impacts on hydrological regime in Europe.

Clim. Past Discuss., doi:10.5194/cp-2016-53, 2016
Manuscript under review for journal Clim. Past
Published: 26 May 2016

1. Introduction

Fundamental for life, precipitation also plays a fundamental role in the redistribution of energy in the atmosphere as ~37% of the solar energy influx into the Earth's atmosphere is involved in the evaporation–condensation–freezing cycle. Highly variable in space, time and intensity, the emission of aerosols by volcanic eruptions may result into dramatic changes in precipitation patterns with large disagreement among models. It is widely accepted that global precipitation decreases one to two years after large explosive volcanic eruptions (Broccoli et al., 2003; Trenberth and Dai, 2007; Gu et al., 2007; Schneider et al., 2009; Gu and Adler, 2011; Iles et al., 2013). The decrease in global mean precipitation by volcanic aerosols is explained by the stabilization of the atmosphere due to the reduction of short-wave radiation reaching the surface thus resulting in a reduction of the evaporation (Bala et al., 2008; Cao et al., 2012). In addition, global circulation changes induced by sulphur-rich eruptions may also result into complex precipitations variations on a regional scale (e.g. in monsoon regions), with seasonal precipitation changes not yet well constrained by climate models. (Gu and Adler, 2011; Joseph and Zeng, 2011; Cao et al., 2012). Concerning the dynamics of volcanic forcing on seasonal and regional precipitation patterns, aerosols may produce slow or fast effects on hydrological cycle depending on whether ocean-atmosphere dynamics are involved or not (Rosenfeld et al., 2008). The fast effect of aerosol forcing, mostly related to solar radiation and cloud physics, has been investigated in more detail (Iles et al., 2013). On the other hand, the physical mechanisms of ocean-atmosphere interaction driving the slow effects (i.e., changes in seasonal and/or regional distribution of precipitation) are still poorly understood (Joseph and Zeng, 2011). In this perspective, evaluating the intensity of the effects of volcanic SO_2 conce.ntrations on hydrological cycle in different Europe climate zones may provide the needed evidence to support modelling work.

Here, we examine rainfall and river flow regimes since the second half of the 19th century in different European climate zones, as they relate to variations in volcanic SO_2 concentrations in the atmosphere. Specifically, we analyse short-term changes of river flows and rainfall regime in order to evaluate quantitatively the effects of sulphate aerosols on extreme precipitation, streamflow events and on hydrological cycle dynamics in Europe.

Clim. Past Discuss., doi:10.5194/cp-2016-53, 2016
Manuscript under review for journal Clim. Past
Published: 26 May 2016

Climate of the Past Discussions
Open Access

Precipitation and river flow data sets are analysed separately in four main climate zones (Schneider et al., 2013) i.e., Mediterranean (MED), Temperate continental (TEMC), Temperate transition (TEMT) and Temperate oceanic (TEMO) zones (Fig.1). The trigger mechanism for extreme hydrological events by sulphur-rich eruptions may involve the radiative forcing of sulphate aerosol over North Atlantic, as evidenced by anomalies in North Atlantic sea surface temperature (SST) and in North Atlantic Oscillation values recorded after sulphur-rich eruptions since 1850 AD.

2. Dataset and analysis

The analysed sulphate aerosol record (1850-1985 period), with an annual resolution based on layer counting, derives from Greenland ice core analysis (Meese et al., 1997) in the context of the Greenland Ice Sheet Project 2, (GISP2; Fig.1).The sulphate dataset clearly record the thirteen VEI≥5 eruptions occurred on a global scale over the same time period (Zielinski, 1995). The clear signatures of Icelandic sulphur-rich eruptions are also well documented in the GISP2 record; the 1970 Hekla VEI3 eruption produced the highest SO_2 peak (i.e., 88 ppb) over the whole time series.

Rivers daily discharge data are from BfG Global Runoff Data Center and from local governmental Institutions (Table 1); daily rain data are from NOAA Global Historical Climatology Network. Specifically, for the MED climate zone, we examine the Tiber River and the Collegio Romano rain gauge, for the TEMC zone, the Nemunas River and the Vilnius Rain gauge, for the TEMT zone, the Elbe River and the Kremsmuenster rain gauge, for the TEMO zone, the Thames River and the Armagh rain gauge (Fig. 1, Table 1).

Although the impact of strong volcanic SO_2 emissions on rainfall intensities and flash floods are still poorly known, the land precipitation responses, in terms of monthly or yearly amounts, to volcanic aerosols are reported to be significant from 1 to 3 years (Bala et al., 2008). In particular, the maximum land mean precipitation reduction after volcanic eruptions, as revealed by latent heat flux anomaly, occurs about 12 months after the maximum reduction in the shortwave flux (Church et al., 2005). On this basis, we average rainfall intensities response across multiple sulphate peaks beyond a fixed threshold through a superposed epoch analysis. Specifically, we relate the annual SO_2 concentrations to the intensities of the twenty-five (ERE_{25}) and ten (ERE_{10}) most intense precipitation episodes, recorded during year +1, as expressed in millimetres per 48 hours. Then, we average ERE_{25} data within two classes of SO_2 concentrations, i.e., years with no detectable SO_2 and years with $SO_2 \geq 20$ ppb. After that, the relationship between annual SO_2 record and rainfall and streamflow records during year +1 is considered.

A Monte Carlo technique was applied to asses the significance of the changes in extreme rainfall intensities as a function of atmospheric SO_2 concentrations and to filter possible effects of multiyear trends. Missing values of rainfall records were also assigned as missing values in the Monte Carlo simulations. The statistical significance of the rainfall intensity changes, ERE_{25} and ERE_{10}, after SO_2-rich eruptions was evaluated by replacing observed rainfall records with data from randomly selected years through 10,000 iterations. Mean ERE_{25} and ERE_{10} values were calculated from all years following sulphur-rich eruptions associated to SO_2 concentrations above 40 ppb in the GISP2 record (Fig.2). Then, the obtained mean ERE_{25} and ERE_{10} values were compared with results from Monte Carlo simulations (10,000 iterations). The *p* values associated to rainfall intensities changes after sulphur-rich eruptions is defined as the probability that the observed pattern of ERE_{25} and ERE_{10}, within individual climatic zones may derive from a random sampling of the rainfall historical record. Thus, *p* values provide a quantitative estimation of the significance of the detected relationship between SO_2 concentrations on rainfall intensities. For each climate zone, the number of years with high-SO_2 concentrations within each record and results from statistical analysis are summarised in Table 2.

The analysis of river streamflows is based on daily flow datasets for the Tiber, Nemunas, Elbe and Thames rivers to calculate extreme day-to-day river flow increases (ΔQ_{day}; Table 1). Specifically, for each year, ΔQ_{day} is defined as the 90th percentile of day-to-day streamflow changes. All the considered rivers are characterised by dam systems for the mitigation of flooding episodes in urbanised areas with potential effects on the analysed ΔQ_{day} values. Thus, for each river drainage basin, we evaluated quantitatively the effects of dam on the streamflow analysis with a statistical approach: concerning the Tiber river, since 1921, (i.e., the starting point of present MED river flow analysis; Table 1), a possible

Clim. Past Discuss., doi:10.5194/cp-2016-53, 2016
Manuscript under review for journal Clim. Past
Published: 26 May 2016

change-point in the flood record at the Ripetta hydrometric gauge took place in 1965, thus possibly affecting ~31% of the total duration of the record. In fact, the Corbara dam, the most important artificial structure to protect Rome from floods, operates since 1965 with a water reservoir of 0.17 km^3 of active storage and a catchment area of 6,070 km^2. The Corbara dam, by delaying the arrival time of flood waves from the upper Tiber, prevents the superposition of flood waves so that the resulting flood waves can be smoothed (Natale and Savi, 2007; Villarini et al., 2011)

In the Nemunas river, ice break-up events, rather than rainfall intensities, are the most important controlling factor the discharge rate peaks. Long-term trends (1812-2006) indicate that in the nineteenth century, ice cover remain unbroken on average for 30 days longer than in the twentieth century (Stonevičius et al., 2008). Moreover, the construction of the Kaunas Hydro Power Plant in 1959, recognised as the to the most impacting dam on the Nemunas ice processes, decreased ice duration between 5 and 15 days on average (Stonevičius et al., 2008).

The dominant flood threat for the Thames River, under favourable atmospheric conditions, derives from surge tides. A complex system of embankments and floodwalls defends London from the tidal regime. In recent times, re-profiling of beds and improvements to the efficiency of weirs resulted in fewer floods in the lower Thames (Bell et al., 2012). To note, we analysed the flow record at Teddington, the principal gauging station on the River Thames, located at the tidal limit. The progressive construction of dams and embankments on Elbe river (both in Czech Republic and Germany) and its tributaries (Vltava and Saale in the Thuringian Forest) over the last two centuries makes difficult the definition of specific major changing points in the day-to-day peak discharge series. A further element of uncertainties in the streamflow record is determined by outflows and inundations occurring as consequence of dike breaches during floods; (e.g., during the May-June 2013 flood in central Europe when diffuse dike breaches took place along the Elbe river). On the other hand, the role of tidal ranges on Elbe streamflow strongly decreases in the upstream direction with no effect at the Neu-Darchau station (Table 1), about 220 km from the Elbe mouth. To note, the middle Elbe part, including the Neu-Darchau station, is considered as a semi-natural river without any river-regulating dams (Haberlandt et al., 2001).

Clim. Past Discuss., doi:10.5194/cp-2016-53, 2016
Manuscript under review for journal Clim. Past
Published: 26 May 2016

Given the possible presence of changing points daily river flow records, firstly we analysed the ΔQ_{day} time series of Tiber, Nemunas, Thames and Elbe rivers through the Mann–Whitney approach (see Additional Informations). From *p* obtained in the Mann–Whitney statistical analysis (see Methods), we detected two main change points; the first concerns the Tiber river with a change point (p~0.02) of ΔQ_{day} time series in 1965. The second change point (p~0.04) is detected in the Nemunas river ΔQ_{day} time series in 1959. No changes points were detected in the Thames and Elbe streamflow records. When no statistically significant change-points are evidenced, we performed the ΔQ_{day} analysis, as related to sulphate aerosol atmospheric records, over the entire record. On the other hand, for the Tiber and Nemunas records, we split the record into two sub-series (i.e, before and after the change-point); then we performed the $\Delta Qday$ analysis of the sub-series separately (table 3).

The statistical significance of the ΔQ_{day} *vs.* sulphate concentrations relationship was derived by applying the Monte Carlo method; specifically, the statistical analysis is based on 10,000 iterations, by randomly sampling a number of SO_2 concentration value from the historical record per iteration as the number of years within each quintile class (i.e., 20% of years of the entire record). For each randomised quintile class, the mean SO_2 value is calculated (Fig.3). Then, we evaluated quantitatively the probability, *p*, that the difference of SO_2 concentrations between the first and the fifth ΔQ_{day} quintile in the historical record may derive from a random sampling of the SO_2 record. For the Tiber and Nemunas rivers, we analysed separately the two subseries after the detected changing points in 1965 and 1959, respectively. The subseries analysis gives level of significance $p<0.05$ for the Tiber River and $p<0.02$ for the Nemunas rivers, thus excluding statistically significant effects of change points on the ΔQ_{day} vs. SO_2 concentrations relationship (results in Table 3).

The Monte Carlo method was applied by assigning the pertinent SO_2 concentration value (i.e., mean of the annual concentration values recorded during the earlier year) to the first (lowest ΔQ_{day} values) and to the fifth (highest ΔQ_{day} values) quintiles interval obtained from the 10,000 iterations. The null hypothesis of no changes of ΔQ_{day} values as a function of SO_2 concentrations is verified from the width of the SO_2 concentration ranges within randomised quintile classes.

The radiative forcing of sulphate aerosol over North Atlantic after sulphur-rich eruptions was evaluated by considering seasonal SST and NAO variations since 1850 as a function of SO_2 concentrations in the GISP2 record. Multiyear NAO trends are filtered by normalising, within each year, the January to December monthly values between 0 and 1. The SST and NAO datasets are available at *www.esrl.noaa.gov* and *www.cpc.ncep.noaa.gov*, respectively.

3. Results

Figure 2 shows the response of ERE_{25} intensities to increasing SO_2 concentrations in the different European climate zones. In the MED area, years with $SO_2 \geq 20$ ppb are characterised by ERE_{25} intensities higher by 13.5 mm on average (standard deviation of the mean, σ_m, 0.8; $p<0.03$) with respect to pristine atmosphere years. In the TEMO zone, SO_2 polluted conditions are associated with an increase of ERE_{25} intensities by 13.1 mm on average ($\sigma_m=2.6$; $p<0.01$). By contrast, in the TEMC zone, the values of ERE_{25} decrease by 11.9 mm on average ($\sigma_m=2.7$; $p<0.19$). This trend is similar to that recorded in the TEMT zone, where ERE_{25} decreases by 16.0 mm on average ($\sigma_m=2.9$; $p<0.13$). To note, when considering the most intense ten precipitation episodes, ERE_{10}, the effects of SO_2 concentrations appear even more pronounced; in fact, in the MED area ERE_{10} intensities increase by 13.9 mm on average ($\sigma_m=1.9$; $p<0.13$), while in the European temperate oceanic zone they increase by 21.9 mm ($\sigma_m=5.3$; $p<0.01$). A more pronounced trend concerns the ERE_{10} values both in the TEMC zone (ERE_{10} = -23.8 mm; $\sigma_m=3.9$; $p<0.16$) and in the TEMT zone (ERE_{10} = -19.9 mm; $\sigma_m=2.6$, $p<0.16$). This general trend in rainfall intensity anomalies is relatively more evident when considering the effects of single large volcanic eruptions; for example one year after the VEI6 1883 Krakatoa eruption, ERE_{10} values in the TEMO zone was affected by a +58.6 mm ($\sigma_m=9.2$) change, with respect to pristine atmosphere years (Fig.2). By contrast, in the TEMC and TEMT zones, ERE_{10} intensities changed by -62.3 mm ($\sigma_m=7.5$) and -95.9 mm ($\sigma_m=13.8$), respectively.

Now, we consider an independent dataset to verify if the observed SO_2-induced rainfall extreme anomalies may have also induced detectable short-term effects on European rivers flow regime. We analysed the daily streamflow data since the second half of the

19th century into the four European climate zones (Fig.1). In Figure 3, the plot of trends was conducted by averaging the SO_2 concentration values (i.e., mean of the annual concentration values recorded during the year preceding SO_2 peaks within fixed concentration thresholds) to each ΔQ_{day} quintile interval. Results show that in the MED, European TEMO and TEMC zones, ΔQ_{day} values increased significantly for increasing values of atmospheric SO_2. Specifically, in the TEMO zone, the increase of SO_2 annual mean concentrations from 11.9±3.5 to 28.5±7.6 ppb is followed by a factor ~2.3 ΔQ_{day} increase. This trend is even more marked in the MED region, where an increase of SO_2 by a factor ~2.4 is followed by a factor >4 enhancement of ΔQ_{day}. Even in the TEMC zone the response of flow regime to increasing SO_2 concentrations shows a similar trend, with an increase of ΔQ_{day} by a factor ~4.6 following an increase of SO_2 by a factor ~4.3. By contrast, in the TEMT zone, to an increase of SO_2 by a factor ~4 corresponds a net decrease of ΔQ_{day} by a factor ~3. The statistical significance of the river flow changes, ΔQ_{day} values, as a function of SO_2 concentrations is summarised in table 3.

4. Discussion

Overall, it appears that, the response of rainfall and streamflow intensities to atmospheric SO_2 concentrations defines a composite yet coherent geographical pattern in Europe. In fact, after sulphur-rich eruptions, both rainfall and flash-flood intensities increase significantly in the MED and TEMO zones, whilst an opposite trend is observed in the TEMT zone. The TEMC zone represents an interesting exception, with a clear discrepancy between the decrease of rainfall intensities and the increase of extreme streamflow episodes following intense SO_2 peak concentrations. We note that annual discharge rate peaks of the Nemunas River are mostly controlled by ice break-up events rather than by rainfall intensities (Yoo and D'Odorico, 2002). Thus, the inconsistency between rainfall intensities and river flow regimes might be related to some effect of atmospheric SO_2 concentrations on ice break-up events. In this perspective, it is widely accepted that premature ice break-up events are associated with relatively more rapid runoff, usually due to a combination of rapid melt and heavy rain (Beltaos and Prowse, 2001). Interestingly, after sulphur-rich eruptions associated to SO_2 concentration values higher than 40 ppb in the

GISP2 record (twelve events since 1850) we found significant warmer temperatures of the atmosphere in late winter and early spring in the TEMC zone (Fig.4). This atmospheric warming is associated to a shift of ice break-up to early dates (i.e., by ~10 days, on average), as revealed by spring discharge rate peaks in the Nemunas hydrograph. Notably, the timing of ice break-up in northern Europe has been related to large-scale atmospheric circulation processes over North Atlantic, as also evidenced by its close relationship with the NAO (Livingstone 1999; Yoo and D'Odorico, 2002)

This picture suggests that the influence of sulphur-rich eruptions on the timing of ice breaks and, more in general, on extreme hydrological events in Europe, can be related to continental scale phenomena rather than to local-scale effects of SO_2 on hydrological cycle dynamics.

5. Conclusions

We found that, since 1850, high SO_2 atmospheric concentrations are followed, during year +1, by significant delayed responses of both the North Atlantic SST and NAO index (Fig.5). This finding suggests a radiative forcing effect of sulphur-rich eruptions, as we found that the twelve most intense SO_2 peaks (i.e., >40 ppb) since 1850 AD are followed, during the year +1, by a North Atlantic SST negative summer anomaly up to ~0.1 °C. This anomaly is followed, within 2-3 months, by a negative NAO phase. In addition, a clear NAO positive phase is observed in February-March of the year +1. Interestingly, the magnitude of positive and negative NAO anomalies increases for increasing SO_2 concentrations (Fig.5).

Although low latitude eruptions are reported to weakly enhance the NAO with relatively warmer winter in the northern hemisphere (Robock and Mao, 1992; 1995; Stenchikov et al., 2002; Hegerl et al., 2011) the response of NAO to sulphur-rich eruptions is not clearly solved by climate models (Driscoll et al., 2012; Charlton-Perez et al., 2013). In this regard, the Atlantic sea surface temperature (SST) is one of the most important governing factors for the NAO and the atmosphere dynamics over most parts of the Northern Hemisphere (Hurrell, 1995). Moreover, the lagged decrease of the NAO index following SO_2-induced negative SST anomalies is coherent with the reported lagged covariability between monthly SST and NAO (Czaja and Frankignoul, 2002; Wang et al., 2004). Negative NAO phases corresponds to relatively weaker westerlies in the TEMC and TEMT zones with a tendency toward blocking and greater frequency of meridional winds (Dettinger and Diaz, 2000; Wang et al., 2004). Under these blocked conditions, storms are steered toward northern Europe or else directly into southern Europe; as a result, rainfall and streamflow can be lowered over central Europe with negative NAO index. By consequence, in the MED zone, negative NAO is associated to moist weather, as recorded by an increase in river flow (Trigo et al., 2002; 2004). Regarding the TEMO zone, significant negative correlations between NAO and regional rainfall amounts were observed in southern England (Wilby et al., 1997) while positive correlations found in Scotland suggest a non homogeneous geographical response of hydrological cycle to atmospheric circulation.

We propose a teleconnected mechanism for volcanically induced extreme hydrological events in Europe. Specifically, the triggering mechanism of extreme rainfall and streamflow events in Europe since 1850 after sulphur-rich eruptions can be explained by sulphate aerosol radiative forcing over North Atlantic causing a net decrease of heat exchange between Ocean and atmosphere through evaporation, precipitation and atmospheric-heating processes. The results of this study display how sulphur-rich eruptions have relevant significance in driving the frequency and intensity of rainfall and related floods in Europe, with variable effects in different climate zones. Consequently, volcanic forcing of hydrological cycle dynamics, superimposed to long term effects of the anthropogenic climate change, needs to be addressed carefully in the context of densely populated areas. As a consequence, this work can furnish a starting point for climate modelling investigation, for reproducing past scenario and predictions at local scale and small temporal resolution.

Supplementary informations

Since the exact time of possible changing points on day-to-day peak discharge series of the investigated rivers is unknown, we applied a non-parametric approach (Pettitt, 1979) for determining the occurrence of a change point. This method allows the detection of significant change in the mean of a time series. From the Mann–Whitney statistic $U_{t,N}$, we verified if two

Clim. Past Discuss., doi:10.5194/cp-2016-53, 2016
Manuscript under review for journal Clim. Past
Published: 26 May 2016

Climate of the Past Discussions
Open Access

samples x_1, … , x_t and $x_{(t+1)}$, … , x_N are from the same population. The test statistic $U_{t,N}$ is given by:

$$U_{t,N} = U_{t,-1,N} + \sum_{j=1}^{N} \operatorname{sgn}(x_t - x_j) \text{ for } t = 2, \dots, N$$

The test determines the number of times a member of the first sample exceeds a member of the second sample. The null hypothesis is the absence of one or more changing points. The associated probabilities for the significance testing are given as:

$$Kt = \mathrm{Max}_{1 \leq t \geq N} \left| U_{t,N} \right|$$

and

$$p \cong 2\exp[-6(K_t)^2/(N^3 + N^2)]$$

For $p<0.05$, a significant change point exists and represents the location of the division point of the time series into two subseries.

Clim. Past Discuss., doi:10.5194/cp-2016-53, 2016
Manuscript under review for journal Clim. Past
Published: 26 May 2016

References

Bala, G, Duffy, PB and Taylor, KE (2008) Impact of geoengineering schemes on the global hydrological cycle. Proc. Natl. Acad. Sci. USA, 105(22): 7 664–9

Bell VA, Kay AL, Cole SJ, Jones RG, Moore RJ, Reynard NS (2012) How might climate change affect river flows across the Thames Basin? An area-wide analysis using the UKCP09 Regional Climate Model ensemble Journal of Hydrology 442-443: 89-104.

Beltaos S, Prowse T (2001) Climate impacts on extreme ice jam events in Canadian rivers. Hydrological Sciences Journal 46(1): 157–181

Beltaos S, Prowse T (2001) Climate impacts on extreme ice jam events in Canadian rivers. Hydrological Sciences Journal 46(1): 157–181

Broccoli AJ, Dixon KW, Delworth TL, Knutson TR, Stouffer RJ and Zeng FR (2003) Twentieth-century temperature and precipitation trends in ensemble climate simulations including natural and anthropogenic forcing. J. Geophys. Res. 108(D24): 4798, DOI: 10.1029/2003JD003812

Cao L, Bala G and Caldeira K (2012) Climate response to changes in atmospheric carbon dioxide and solar irradiance on the time scale of days to weeks. Environ. Res. Lett. 7, 034015

Charlton-Perez AJ, et al. (2013) Mean climate and variability of the stratosphere in the CMIP5 models, J. Geophys. Res.,118 (6): 2494-2505, doi:10.1002/jgrd.50125

Church JA, White NJ, Arblaster JM (2005) Significant decadal-scale impact of volcanic eruptions on sea level and ocean heat content. Nature, 438 (7064):74–77

Czaja A, and Frankignoul, C(2002) Observed impact of North Atlantic SST anomalies on the North Atlantic Oscillation, J. Climate, 15: 606-623

Dettinger M, Diaz HF(2000) Global characteristics of stream flow seasonality and variability. Journal of Hydrometeorology 1(8): 289 – 309

Driscoll S, Bozzo A, Gray LJ, Robock A and Stenchikov G (2012) Coupled Model Intercomparison Project 5 (CMIP5) simulations of climate following volcanic eruptions, J. Geophys. Res., 117, D17105, doi:10.1029/2012JD017607

Gu G and Adler R F (2011) Precipitation and temperature variations on the interannual time scale: Assessing the impact of ENSO and volcanic eruptions. J. Clim. 24: 2258–70, doi: http://dx.doi.org/10.1175/2010JCLI3727.1

Gu G J, Adler R F, Huffman GJ and Curtis S (2007) Tropical rainfall variability on interannual-to-interdecadal and longer time scales derived from the GPCP monthly product. J. Clim. 20: 4033–46, doi: http://dx.doi.org/10.1175/JCLI4227.1.

Clim. Past Discuss., doi:10.5194/cp-2016-53, 2016
Manuscript under review for journal Clim. Past
Published: 26 May 2016

Haberlandt U, Klöcking B, Krysanova V, Becker A (2001) Regionalisation of the base flow index from dynamically simulated flow components - A case study in the Elbe River Basin Journal of Hydrology 248(1–4): 35–53.

Hegerl G, Luterbacher J, González-Rouco F, Tett SFB, Crowley T, Xoplaki E (2011) Influence of human and natural forcing on European seasonal temperatures, Nature Geoscience, 4 (2): 99-103

Hurrell JW (1995) Decadal trends in the North Atlantic Oscillation: regional temperatures and precipitation. Science 269:676–679

Iles, CE, Hegerl, G C, Schurer, AP and Zhang X (2013) The effect of volcanic eruptions on global precipitation. J. Geophys. Res. 118(16): 8770–86, DOI: 10.1002/jgrd.50678

Joseph R and Zeng N (2011) Seasonally modulated tropical drought induced by volcanic aerosol. J. Clim. 24: 2045–60, doi: 10.1175/2009JCLI3170.1

Livingstone DM (1999) Ice break-up on southern Lake Baikal and its relationship to local and regional air temperatures in Siberia and to the North Atlantic Oscillation. Limnol. Oceanogr. 44, (6): 1486–1497

Meese DA, Gow AJ, Alley RB, Zielinski GA, Grootes PM, Ram M... & Bolzan, JF (1997) The Greenland Ice Sheet Project 2 depth-age scale: Methods and results. Journal of Geophysical Research: Oceans (1978–2012), 102(C12), 26411–26423.12

Natale L, Savi F (2007) Monte Carlo analysis of probability of inundation of Rome. Environ Model Softw 22(10):1409–1416 doi:10.1016/j.envsoft.2006.12.004

Pettitt A. (1979) A nonparametric approach to the change-point problem. Applied Statistics, 28: 126–135.

Robock A and Mao J (1995) The volcanic signal in surface temperature observations. J. Climate, 8: 1081103

Robock A and Mao J (1992) Winter warming from large volcanic eruptions. Geophys Res Lett 19: 2405–2408

Rosenfeld D, Lohmann U, Raga GB, O'Dowd CD, Kulmala M, Fuzzi S, Reissell A, Andreae MO (2008) Flood or drought: how do aerosols affect precipitation? Science, 321(5894):1309–1313, doi: 10.1126/science.1160606.

Schneider C, Laizè CLR, Acreman MC and Florke M (2013) How will climate change modify river flow regimes in Europe? Hydrol. Earth Syst. Sci., 17: 325-339. doi:10.5194/hess-17-325–2013.

Clim. Past Discuss., doi:10.5194/cp-2016-53, 2016
Manuscript under review for journal Clim. Past
Published: 26 May 2016

Schneider DP, Ammann CM, Otto-Bliesner BL and Kaufman DS (2009) Climate response to large, high-latitude and low-latitude volcanic eruptions in the community climate system model. J. Geophys. Res. 114, D15101

Stenchikov G, Robock A, Ramaswamy V, Schwarzkopf MD, Hamilton K, and Ramachandran S (2002). Arctic Oscillation response to the 1991 Mount Pinatubo eruption: Effects of volcanic aerosols and ozone depletion, J. Geophys. Res., 107 (D24), 4803, doi:10.1029/2002JD002090

Stonevičius E., Stankunavicius G., Kilkus K. (2008) Ice regime Dynamics in the Nemunas River, Lithuania. Climate Research, 36: 17–28

Trenberth KE and Dai A (2007) Effects of Mount Pinatubo volcanic eruption on the hydrological cycle as an analogue of geoengineering. Geophys. Res. Lett. 34, L15702, doi:10.1029/2007GL030524, 2007.

Trigo RM, Osborn TJ, Corte-Real J (2002) The North Atlantic oscillation influence on Europe: climate impacts and associated physical mechanisms. Climate Research 20:9–17, doi:10.3354/cr020009

Trigo RM, Pozo-Vasquez D, Osborn TJ, Castro-Diez Y, Gamiz-Fortis S, Esteban-Parra, MJ (2004) North Atlantic oscillation influence on precipitation, river flow and water resources in the Iberian peninsula, Int. J. Climatol. 24: 925-944. DOI: 10.102/joc.1048.

Villarini G., Smith JA, Napolitano F, Baeck ML (2011) Hydrometeorological analysis of the December 2008 flood in Rome. Hydrological Sciences Journal, 56 (7), 1150–1165

Wang W, Anderson BT, Kaufmann RK, Myeni RB (2004) The relation between the North Atlantic Oscillation and SSTs in the North Atlantic basin. J Clim 17: 4752–4759

Wilby RL, O'Hare G, Barnsley N (1997) The North Atlantic Oscillation and British Isles climate variability, 1865-1996, Weather, 52: 266-276, 9. DOI: 10.1002/j.1477-8696.1997.tb06323.x

Yoo JC, D'Odorico P (2002) Trends and fluctuations in the dates of ice break-up of lakes and rivers in Northern Europe: the effect of the North Atlantic Oscillation. J Hydrol 268:100–11

Zielinski G, (1995) Stratospheric loading and optical depth estimates of explosive volcanism over the last 2100 years derived from the Greenland Ice Sheet Project 2 ice core J. Geophys. Res., 100(D10), 20937–20955, doi:10.1029/95JD01751

Clim. Past Discuss., doi:10.5194/cp-2016-53, 2016
Manuscript under review for journal Clim. Past
Published: 26 May 2016

Climate of the Past Discussions
Open Access

404 **Figures**

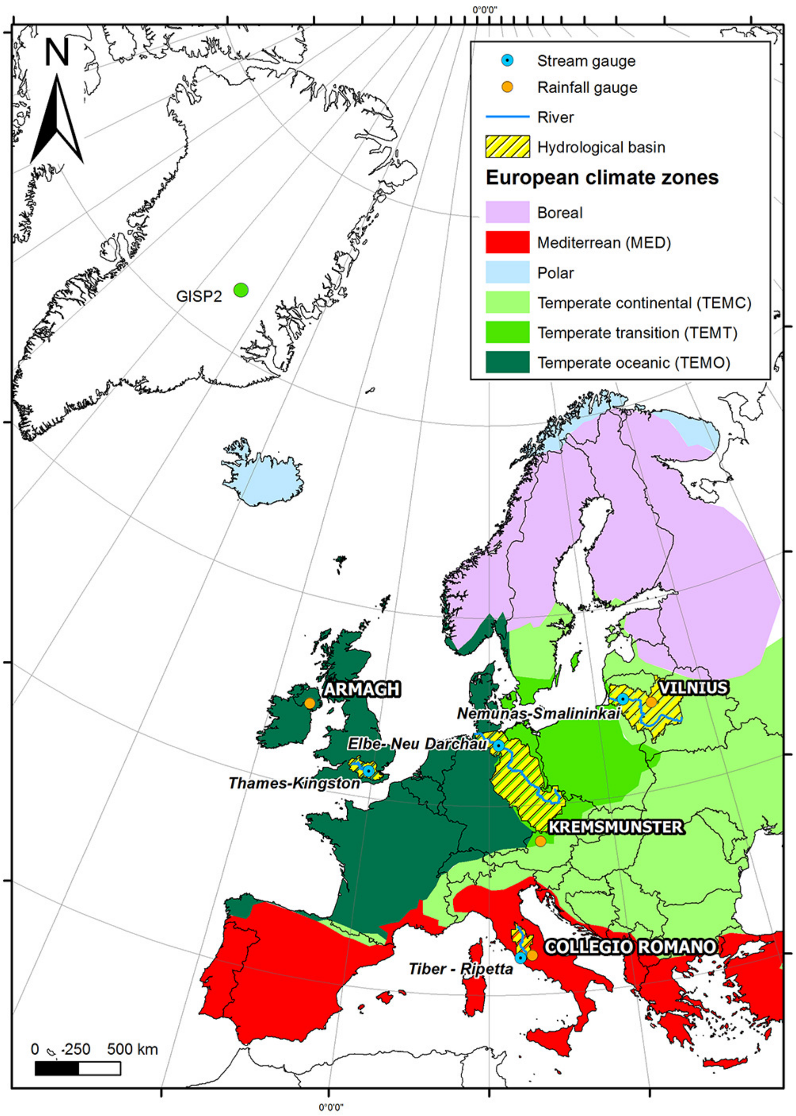

405

406

407 **Figure 1: Location of hydrometric and rainfall gauges considered in the present study**; the six European

408 climate zones (Meese et al., 1997) are also shown.

Clim. Past Discuss., doi:10.5194/cp-2016-53, 2016
Manuscript under review for journal Clim. Past
Published: 26 May 2016

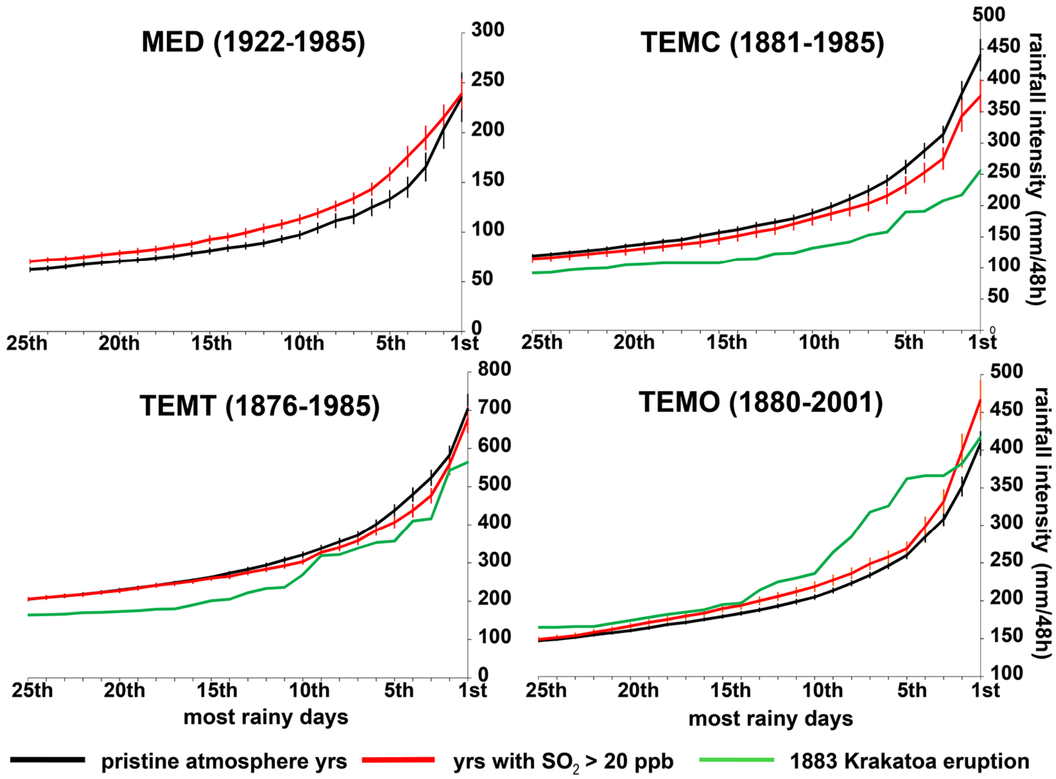

Figure 2: Intensities of the 25 most rainy days (ERE_{25}) for years with no detectable volcanic SO_2 (black line) and years with SO_2≥20 ppb (red line). Vertical bars are the standard deviations of the mean. Concentrations of volcanic aerosols above 20 ppb are associated to a significant increase of the ERE_{25} intensities both in the MED area (mean value +10.7% at Collegio Romano rain gauge) and in the TEMO climatic zone (+1.4% at Armagh rain gauge) with respect to pristine atmosphere years. By contrast, in the TEMC (Vilnius rain gauge) and in the TEMT (Kremsmunster rain gauge) climatic zones, ERE_{25} values decrease by 3.2 % and by 5.2 % on average, respectively. This general trend is more pronounced after large eruptions as, for example, after the 1883 VEI6 Krakatoa eruption (green line). SO_2 concentrations derive from GISP2 Greenland ice core record.(Schneider et al., 2013).

Clim. Past Discuss., doi:10.5194/cp-2016-53, 2016
Manuscript under review for journal Clim. Past
Published: 26 May 2016

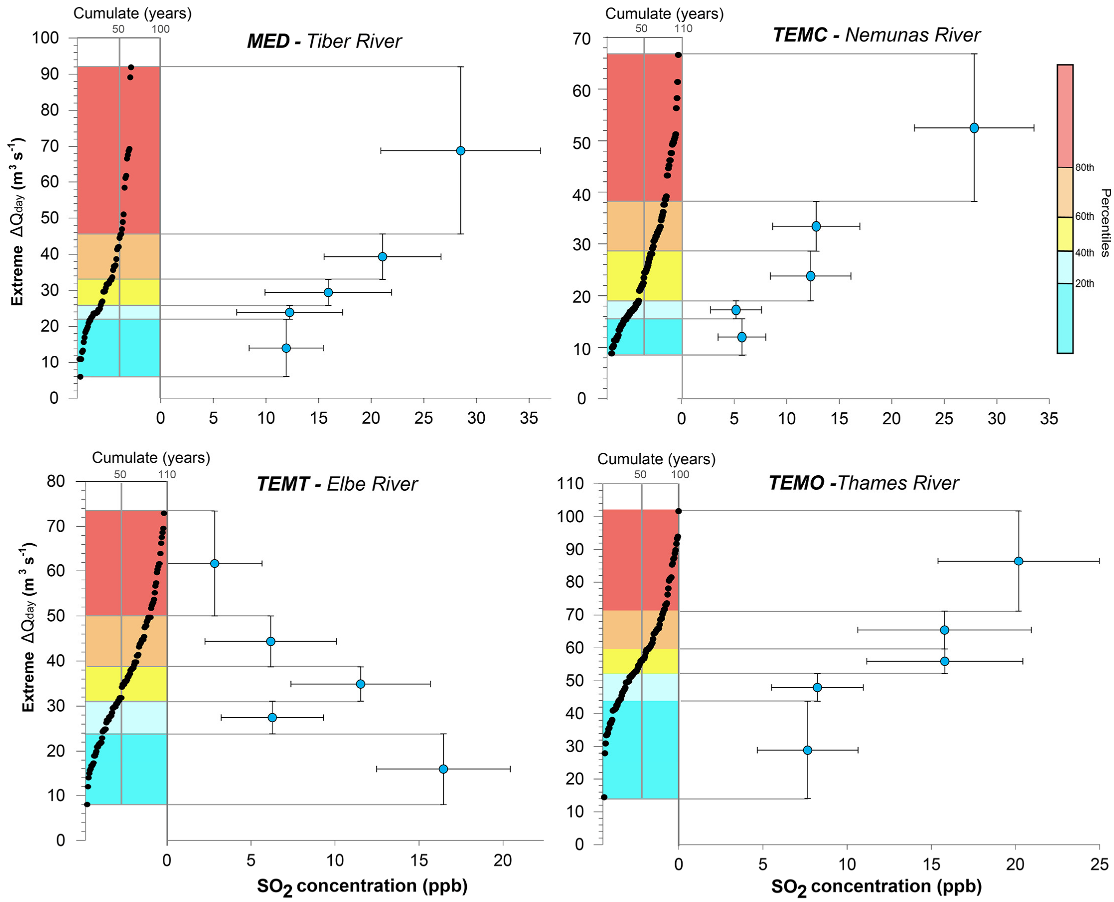

Figure 3. Extreme day-to-day river flow increases (ΔQ_{day}) vs. SO_2 concentrations in Greenland ice core records (GISP2). The Probability Distribution Function (PDF, black dots) of ΔQ_{day} values was divided into five equal-sized groups (quintiles) and ordered from low to high ΔQ_{day} values. SO_2 concentration values are the mean of the annual concentrations as determined within each ΔQ_{day} quintile interval.

Clim. Past Discuss., doi:10.5194/cp-2016-53, 2016
Manuscript under review for journal Clim. Past
Published: 26 May 2016

Climate of the Past Discussions

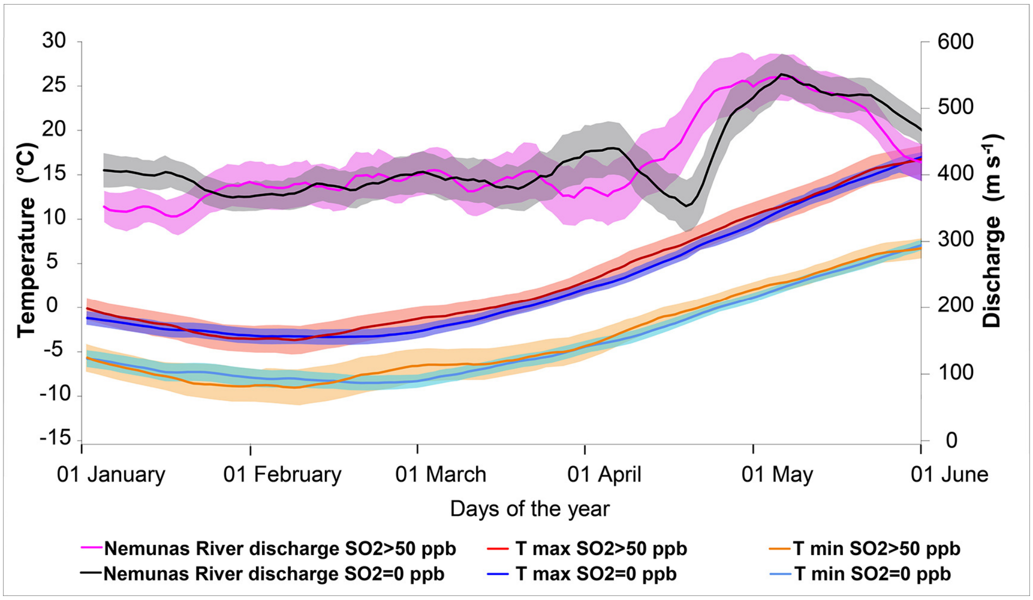

Figure 4: Impact of volcanic SO_2 on the timing of ice breaks at the Nemunas River. Nemunas River discharge at Smalininkai stream gauge (m^3 s^{-1}) and maximum and minimum atmospheric temperatures at Vilnius (°C), for years with SO_2>50 ppb, years with SO_2=0 (pristine atmosphere). Both maximum and minimum temperatures show an increased trend during years with SO_2>50 ppb, with respect to pristine atmosphere years. The trend of discharge for years with SO_2>50 ppb clearly shows earlier dates for maximum flows, due to an earlier ice-break up, with respect to years with pristine atmosphere. Shaded areas are the standard deviation of the mean. Data source are reported in the text.

Clim. Past Discuss., doi:10.5194/cp-2016-53, 2016
Manuscript under review for journal Clim. Past
Published: 26 May 2016

Climate of the Past Discussions

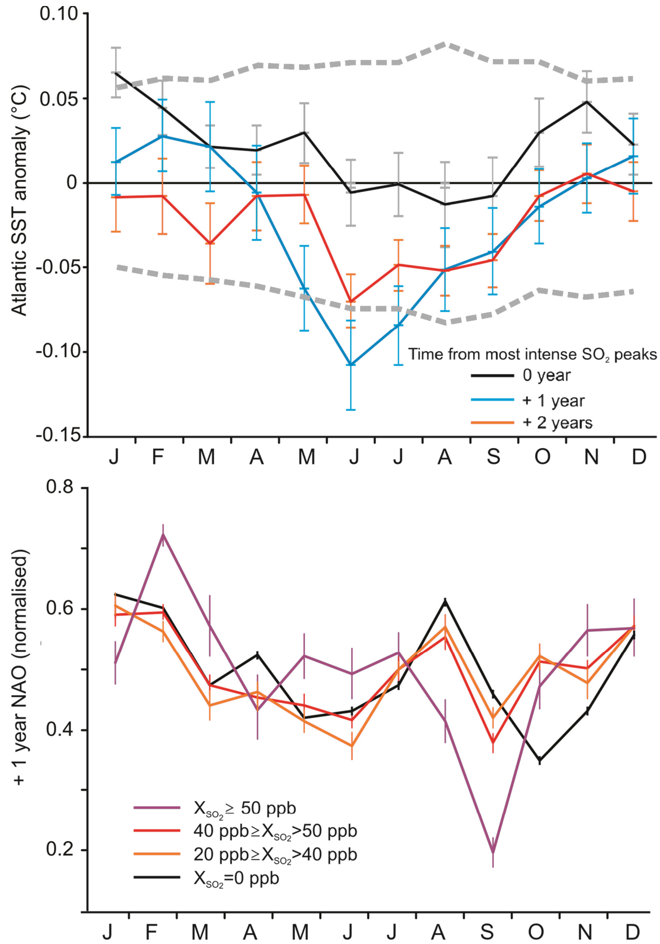

Figure 5: **Monthly impact of volcanic sulphate aerosols on Atlantic Sea Surface temperature (SST) and NAO index since 1850.** Post-volcanic Atlantic SST anomalies produced by the twelve most intense SO_2 peaks in the GISP2 record (i.e., $SO_2 \geq 40$ ppb compared with SO_2 = 0 ppb). Curves represent lag 0, lag +1 and lag +2 years, respectively, from sulphate peaks. Dashed lines denote the 1σ standard deviation from the monthly mean values over the entire record (upper). Sensitivity of NAO (normalised values) to increasing SO_2 concentrations values (lag +1 year) (lower). Vertical bars are the standard deviations of the mean.

Clim. Past Discuss., doi:10.5194/cp-2016-53, 2016
Manuscript under review for journal Clim. Past
Published: 26 May 2016

Table 1. Dataset, periods, hydrometric and rain gauge stations and references considered in the river flow and rainfall analyses.

Climate zone	Period	Missing years	Station (*Country*)	Hydrometric (H) Rain gauge (R)	References
MED	1922 - 1985	1928; 1934; 1937; 1941	Collegio Romano (*Italy*)	R	*
	1921 - 1985	1984	Ripetta (*Italy*)	H (Tiber River)	**
TEMC	1881 - 1985	1915-17; 1943-44	Vilnius (*Lithuania*)	$R^{\#}$	***
	1877 - 1985	1930-32; 1943-45	Smalininkai (*Lithuania*)	H (Nemunas River)	**
TEMT	1876 - 1985	-	Kremsmuenster (*Austria*)	R	***
	1875 - 1985	-	Neu-Darchau (*Germany*)	H (Elbe River)	**
TEMO	1880 - 1985	-	Armagh (*United Kingdom*)	R	***
	1883 - 1985	-	Kingston (*United Kingdom*)	H (Thames River)	**

Notes:

** Ufficio Idrografico e Mareografico Regione Lazio [UIRL], Centro Funzionale (http://www.idrografico.roma.it/)*

*** Global Runoff Data Centre [GRDC]. Koblenz, Federal Institute of Hydrology (BfG), (2014).*

**** Global Historical Climatology Network [GHCN],NOAA Satellite and Information Service,*

$R^{\#}$ Temperature analysed in figure 4 are from the Vilnius station.

Clim. Past Discuss., doi:10.5194/cp-2016-53, 2016
Manuscript under review for journal Clim. Past
Published: 26 May 2016

Climate of the Past Discussions

Table 2. Statistical significance of the effects of SO_2 on rainfall intensities from Monte Carlo method. Within individual climate zones, the number of years with high-SO_2 concentrations (≥40 ppb) corresponds to the number of randomly selected years within the GISP2 record for Monte Carlo simulations (10^4 iterations).

Climate zone	Station (*Country*)	Record duration yrs (missing yrs)	yrs with SO_2 ≥40 ppb	p (ERE_{25})	p (ERE_{10})
MED	Collegio Romano (*Italy*)	65 (*4*)	9	<0.03	<0.13
TEMC	Vilnius (*Lithuania*)	106 (*5*)	12	<0.19	<0.16
TEMT	Elbe (*Germany*)	111 (*0*)	12	<0.13	<0.16
TEMO	Thames (*UK*)	107 (*0*)	12	<0.01	<0.01

Table 3. Results from Monte Carlo method for the statistical significance of the effects of SO_2 on streamflow extreme events.

Climate zone	River (*Country*)	Record duration yrs (*missing yrs*)	Mean SO_2 concentration (σ_m) in ppb		*p*
			ΔQday lowest (1st) quintile	ΔQday highest (5th) quintile	
MED	Tiber (*Italy*)	65 (*1*)	11.9 (*3.5*)	28.5 (*7.6*)	<0.01
TEMC	Nemunas (*Lithuania*)	109 (*6*)	6.1 (*2.3*)	28.2 (*5.7*)	<0.001
TEMT	Elbe (*Germany*)	110 (*0*)	7.6 (*3.0*)	20.1 (*4.8*)	<0.01
TEMO	Thames (*UK*)	103 (*0*)	18.2 (*4.0*)	4.6 (*2.8*)	<0.02